A DFT Study of the Molecular Mechanisms of the Diels−Alder Reaction between Cyclopentadiene and 3-Phenyl-1-(2-pyridyl)-2-propen-1-one − Role of the Zn^{2+} Lewis Acid Catalyst and Water Solvent

Luis R. Domingo,*[a] Juan Andrés,[b] and Claudio N. Alves[b][‡]

Keywords: Catalysis / Cycloadditions / Density functional calculations / Lewis acids / Reaction mechanisms

The molecular mechanism of the Diels–Alder reaction between cyclopentadiene (**1**) and 3-phenyl-1-(2-pyridyl)-2-propen-1-one (**2**) in the absence and in the presence of a Zn^{2+} Lewis acid catalyst has been studied by quantum mechanical calculations at the B3LYP/6-31G* level of theory. A continuum model was selected to represent the effects of the water as solvent. For the uncatalyzed process, two channels, *endo* and *exo*, were characterized, and the mechanism corresponded to an asynchronous concerted reaction associated with a [4+2] process. The presence of a Lewis acid catalyst changed the mechanism drastically, the reaction taking place by a polar stepwise mechanism. In the first step, a C–C sigma bond was formed by the nucleophilic attack of **1** on the conjugate position of the Lewis acid coordinated α,β-unsaturated ketone to give a zwitterionic intermediate, while the second step was a ring-closure process by this intermediate to give the final formally [4+2] cycloadduct. The theoretical results have been compared with available experimental data and an understanding of the role of Lewis acids and water solvent emerges from analysis of the results.

Introduction

The Diels−Alder (DA) reaction represents a most powerful synthetic procedure for the preparation of six-membered cyclic compounds.[1] Given the importance of this reaction, intensive efforts have been directed toward the elucidation of its molecular mechanism, and a plethora of experimental and theoretical studies have appeared in the literature.[2] To be reasonably fast, DA reactions require opposite electronic features in the substituents at the diene/dienophile pair. Lewis acids (LA) are common catalysts for DA reactions, enhancing the reaction rates and producing significant changes in *endo*/*exo*- and regioselectivities in comparison with those of the uncatalyzed processes.[1c,2a]

α,β-Unsaturated carbonyl compounds, as electron-poor dienophiles, are activated by coordination of the carbonyl oxygen atom to a LA catalyst. This coordination polarizes the C−C double bond, increasing the electrophilicity of the β-carbon. Bond-formation at the β-carbon hence preceded that at the α-carbon. Consequently, the reaction mechanism can change progressively from asynchronous and concerted to polar and stepwise with increasing ability of the electron-withdrawing substituent to stabilize a negative charge. The molecular mechanism of an LA-catalyzed DA reaction can therefore be located on the border between highly asynchronous but concerted mechanisms and stepwise processes with a largely ionic character.[3]

Several theoretical works have been devoted to the study of the role of LAs on the molecular mechanisms of cycloaddition reactions.[3−6] These studies indicate that LAs amplify the asynchronicity of the bond-formation process and charge transfer, due to an increase in the electrophilicity of the LA-coordinated dienophile. The corresponding transition states (TSs) have highly polar natures and the formally [4+2] cycloaddition processes become nucleophilic attacks.[5] Although single, highly asynchronous TSs associated with concerted mechanisms have been found for most LA-catalyzed DA reactions,[3,5,6] stepwise mechanisms with the formation of zwitterionic intermediates through an *anti* attack mode are also feasible.[6] However, the *syn* reactive channel is clearly favored over the stepwise *anti* one. In addition, the large barrier associated with the bond-rotation of the *anti* intermediates to perform the ring-closure process means that these intermediates exist in association/dissociation equilibria.[6]

Solvent effects play relevant roles both in the stereoselectivity and in the rates of DA reactions.[5,7] Most of these reactions are carried out in organic solvent because of the low solubilities of the reagents in water.[2a,8] Recently,

[a] Instituto de Ciencia Molecular, Departamento de Química Orgánica, Universidad de Valencia,
Dr. Moliner 50, 46100 Burjassot, Valencia, Spain
E-mail: domingo@utopia.uv.es
[b] Departament de Ciéncies Experimentals, Universitat Jaume I, Box 224, 12080 Castellò, Spain
[‡] On leave from: Departamento de Química, Centro de Ciências Exatas e Naturais, Universida de Federal do Pará, CP 11101, 66075-110 Belém, PA, Brasil

Engberts and co-workers have studied the effects of different divalent cations of first row transition metals as LA catalysts on the rates and *endo*/*exo* stereoselectivities of DA reactions between bidentate dienophiles and cyclopentadiene in water.[9,10] The presence of LAs drastically accelerates the reaction, but the rate-enhancing effect of the water on the catalyzed reaction is less pronounced than the corresponding effect on the uncatalyzed reaction.[10] Moreover, water does not induce any clearly enhanced *endo* selectivity in these reactions.

These experimental studies offered the opportunity to carry out a complementary theoretical analysis in order to compare theory and experiment. In a previous paper we have reported an AM1 study on the molecular mechanisms of the uncatalyzed and Zn^{2+} LA-catalyzed DA reactions between cyclopentadiene (**1**) and the bidentate 3-phenyl-1-(2-pyridyl)-2-propen-1-one (**2**)[11] as model compounds with the main group elements intervening in the DA reactions reported by Engberts et al.;[10] the limitations and weaknesses of this semiempirical method for analysis of this type of chemical reaction were emphasized. We now present the first DFT[12] study of the molecular mechanism of the uncatalyzed and Zn^{2+} LA-catalyzed DA reactions between **1** and **2** (see Schemes 1 and 2). Solvent effects have also been considered, in order to elucidate the role of the water solvent on these LA-catalyzed cycloadditions. Our purpose was to contribute to a better understanding of the mechanistic features of these LA-catalyzed processes, especially through the location and characterization of all stationary points involved in this type of cycloaddition reaction.

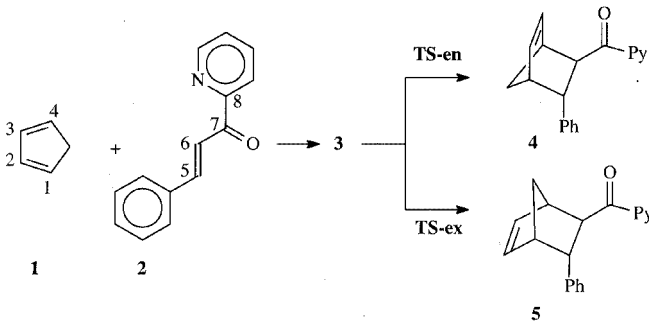

Scheme 1

Results and Discussion

Firstly, the energetic aspects, geometrical parameters of TSs, and their electronic structures in terms of bond orders and natural charges were analyzed for the uncatalyzed process in the gas phase. Next, the role of the LA catalyst was interpreted. The results, including solvent effects, are discussed below.

Study of the Uncatalyzed Cycloaddition Between 1 and 2

Four planar conformations are possible for the α,β-unsaturated ketone **2** due to free rotation about the C6−C7 and C7−C8 bond. These conformations are associated with *s-cis* and *s-trans* arrangements of the α,β-unsaturated ketone and *syn* and *anti* arrangements of the pyridyl nitrogen and the carbonyl oxygen atoms. A conformational analysis for **2** indicated that the *syn* conformations are ca. 8 kcal/mol higher in energy than the *anti* ones because of the strong repulsion between the lone pairs of the oxygen and the nitrogen atoms in the *syn* planar conformation. In addition, the *anti s-trans* conformer is 3.4 kcal/mol higher in energy than the *anti s-cis* one. We consequently chose the *anti s-cis* conformation for **2** in the uncatalyzed study (see Scheme 1).

An exhaustive exploration of the potential energy surface (PES) for the uncatalyzed cycloaddition allowed us to identify several molecular complexes (MCs) associated with very early stages of the reaction and situated in a very flat region determining the access to the different reactive channels. MC formation could take place in different arrangements of the reactants, with quite a large distance (of around 4 Å) between **1** and **2**. Their presence on a very flat surface on the PES made the location of the MC associated with each reactive channel very difficult, and so the most stable MC (**3**) was included (see Figure 1). Its formation occurs with no appreciable barrier, **3** being 0.3 kcal/mol more stable than the separated reactants **1** and **2**.

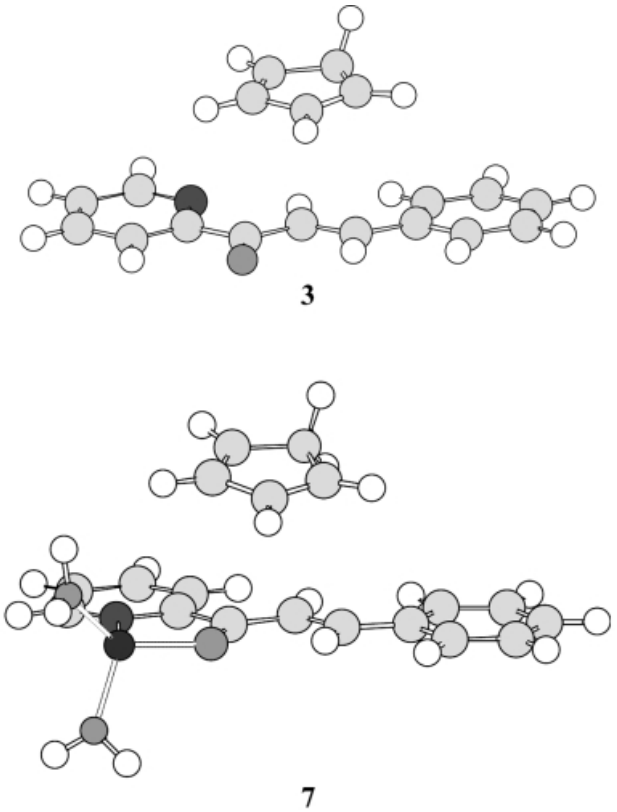

Figure 1. Geometries of the molecular complexes **3** and **7**

The cycloaddition reaction between cyclopentadiene **1** and the α,β-unsaturated ketone **2** can take place by two reaction pathways, corresponding to the *endo* and *exo* approach modes of the 1,3-diene system of **1** to the carbonyl group in **2** (see Scheme 1). Analysis of the results found that the cycloaddition takes place by an asynchronous concerted mechanism associated with a [4+2] process. Thus, an MC (**3**), two TSs (**TS-en** and **TS-ex**), and two cycloadducts (**4** and **5**) corresponding to the *endo* and *exo* channels, respectively, were found and characterized. The stationary points corresponding to the uncatalyzed reaction between **1** and **2** are presented in Scheme 1 together with the atom numbering, while the total and relative energies are summarized in Table 1. The geometries of the MC **3** and the TSs are presented in Figure 1 and 2, respectively.

The values of the relative energies of **TS-en** and **TS-ex** with respect to **3** are 20.7 and 20.4 kcal/mol, respectively. In the gas phase, therefore, this cycloaddition is slightly *exo*-stereoselective. The lengths of the forming C1−C5 and C4−C6 bonds in the *endo* **TS-en** are 2.083 and 2.362 Å, respectively, while the corresponding values in the *exo* **TS-ex** are 2.102 and 2.373 Å, respectively. The extent of the asynchronicity of the bond formation can be gauged by the difference between the lengths of the bonds being formed in the reaction: Δr = d(C4−C6) − d(C1−C5). These values, Δr = 0.27 for **TS-en** and Δr = 0.28 for **TS-ex**, indicate that both TSs correspond to concerted but asynchronous bond-formation processes, whereas the forming C−C bond at the β position of **3** is to a large extent being formed as a consequence of the polarization of the C5−C6 double bond due to the adjacent electron-withdrawing carbonyl group.

Table 1. Total energies (au) and relative energies[a] (kcal/mol, in parentheses) for the stationary points corresponding to the cycloaddition reactions of cyclopentadiene, **1**, with the unsaturated ketone **2**, and with the Zn^{2+} LA coordinated unsaturated ketone **6**, in vacuo and in water, ε = 78.39

	in vacuo		in water	
	uncatalyzed process			
1	−194.101064		−194.105079	
2	−670.078854		−670.100048	
3	−864.180570	(0.00)	−864.200125	(0.00)
TS-en	−864.147555	(20.72)	−864.170146	(18.81)
TS-ex	−864.148002	(20.44)	−864.170125	(18.83)
4	−864.194607	(−8.81)	−864.212003	(−7.45)
5	−864.196532	(−10.02)	−864.213896	(−8.64)
	Zn^{2+} LA catalyzed process			
6	−2601.616118		−2601.877789	
7	−2795.724951	(0.00)	2795.968569	(0.00)
TS1-g1s	−2795.710493	(9.07)	−2795.953896	(9.21)
TS1-g2s	−2795.712518	(7.80)	−2795.947328	(13.33)
TS1-ans	−2795.707344	(11.05)	−2795.948876	(12.36)
TS1-g1r	−2795.710097	(9.32)	−2795.953518	(9.44)
TS1-g2r	−2795.709102	(9.95)	−2795.946834	(13.64)
TS1-anr	−2795.711292	(8.57)	−2795.947123	(13.46)
IN-g1s	−2795.712021	(8.11)	−2795.961954	(4.15)
IN-g2s	−2795.714610	(6.49)	−2795.950076	(11.60)
IN-ans	−2795.713852	(6.96)	−2795.957910	(6.69)
IN-g1r	−2795.713198	(7.38)	−2795.957078	(7.21)
IN-g2r	−2795.713781	(7.01)	−2795.963821	(2.98)
IN-anr	−2795.713156	(7.40)	−2795.955881	(7.96)
TS2-s	−2795.706337	(11.68)	−2795.958294	(6.45)
TS2-r	−2795.707794	(10.77)	−2795.958602	(6.25)
8	−2795.713930	(6.92)	−2796.025138	(−35.50)
9	−2795.717423	(4.72)	−2796.028042	(−37.32)

[a] Relative to the MCs **3** and **7**.

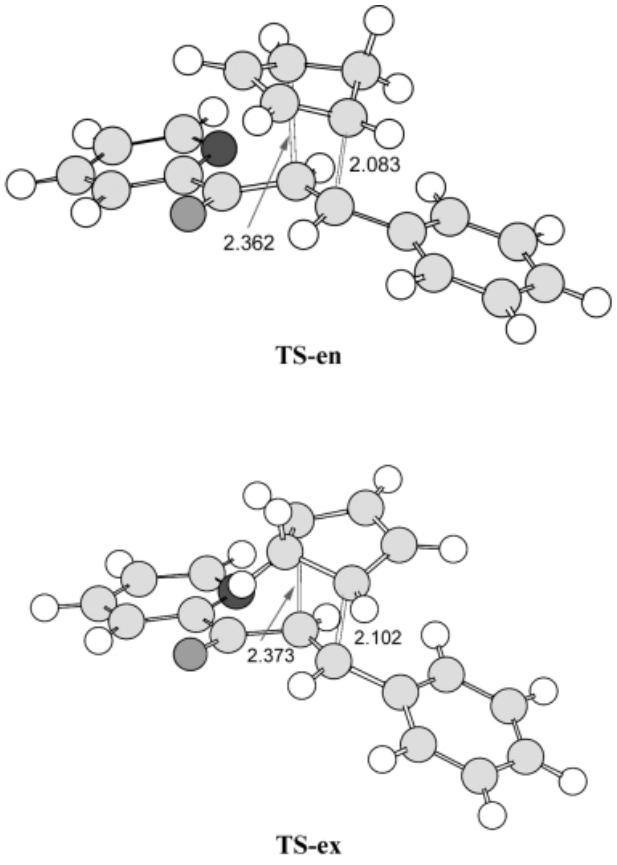

Figure 2. Selected geometrical parameters for the transition structures corresponding to the cycloaddition reaction between cyclopentadiene (**1**) and the unsaturated ketone **2**; the lengths of the bonds directly involved in the reaction are given in angstroms

The extent of bond formation along a reaction pathway can also be described by the concept of bond order (BO).[13] The BO values of the forming C1−C5 and C4−C6 bonds in both TSs are 0.45 and 0.30, respectively. These data show a similar bond formation in both the *endo* and the *exo* reactive channels. Finally, natural population analysis (NPA)[19a] found that the values of the charge transferred from **1** to **3** in both TSs are close to 0.3 e.

Study of the Lewis Acid-Catalyzed Cycloaddition Between 1 and 7

As stated in the introduction, this DA reaction is catalyzed by the presence of divalent cations of the first row transition metals. Our next step was to study the role of these LAs in the reaction, with Zn^{2+} serving as a model system.

An exhaustive exploration of the PES for the LA-catalyzed cycloaddition also allowed us to identify several MCs associated with very early stages of the reaction and located on a very flat surface on the PES. The most stable MC (**7**) was therefore included (see Figure 1). Its formation takes place with no appreciable barrier, **7** being 4.9 kcal/mol more stable than the separated reactants **1** and **6**.

Analysis of the results indicated that the LA-catalyzed cycloaddition takes place by a stepwise process. The first step corresponds to the nucleophilic attack of the end of the 1,3-diene system of **1** (atom C1) at the β-position of the LA-coordinated unsaturated ketone **6** (atom C5), to give an acyclic zwitterionic intermediate (IN). This nucleophilic attack corresponds to a one-center addition. As C1 and C5 are prochiral carbon atoms, two pairs of enantiomeric approach modes are possible. Only the attack modes resulting from the approach of **1** by its *si* and *re* faces to the *si* face of **6**, named as *s* and *r*, respectively, were considered. In addition, three staggered conformations of **1** relative to **6** around the forming C1−C5 bond in these stereoisomeric attack modes are feasible. These could be associated with the τ dihedral angle defined by the C2−C1−C5−C6 atoms: two *gauche* (*g1* and *g2*, with a value of τ close to ±60°) and one *anti* (*an*, with a value of τ close to 180°). Six reactive channels and their enantiomeric counterparts are therefore feasible for this one-center addition (see Scheme 2). From the **IN-g1s** and **IN-g1r** intermediates, a ring-closure process associated with C4−C6 bond formation produces the final *endo* and *exo* formal [4+2] cycloadducts **8** and **9**, respectively. Finally, the *an* and *g2* intermediates can be related to the *g1* ones through a C1−C5 bond rotation.

The stationary points corresponding to the LA-catalyzed cycloaddition reaction between **1** and **6** are presented in Scheme 2 together with the atom numbering, while the total and relative energies are summarized in Table 1. The geometry of MC **7** is given in Figure 1, while the geometries of the TSs in the stepwise process are presented in Figures 2 and 4. The following stationary points were characterized: an MC (**7**), six TSs corresponding to the one-center addition with the C1−C5 bond formation (**TS1-g1s**, **TS1-g2s**, **TS1-ans**, **TS1-g1r**, **TS1-g2r**, and **TS1-anr**), the corresponding six zwitterionic intermediates (**IN-g1s**, **IN-g2s**, **IN-ans**, **IN-g1r**, **IN-g2r** and **IN-anr**), two TSs associated with the ring-closure processes with C4−C6 bond formation (**TS2-s** and **TS2-r**), and two cycloadducts (**8** and **9**, see Scheme 2).

Analysis of the energies of the TSs associated with the one-center addition showed that they lie in a narrow range (3.3 kcal/mol). While for the *s* channels the most favorable attack corresponds to the *g2* approach mode, via **TS1-g2s**, for the *r* channels the most favorable attack corresponds to the *an* approach mode, via **TS1-anr**, with formation of the acyclic intermediates **IN-g2s** and **IN-anr**, respectively. Formation of the final cycloadducts **8** and **9** demands a ring closure of these acyclic intermediates. However, while the ring-closure of the *g1* intermediates **IN-g1s** and **IN-g1r** takes place in a single step with a very low barrier (ca. 3.5 kcal/mol), a C1−C5 bond rotation is necessary for the acyclic intermediates **IN-g2s** and **IN-anr** to carry out the subsequent C4−C6 bond formation. In consequence, the feasibility of the *g2s* and *anr* reactive channels depends on the relative energies of the TSs associated with the one-center addition (**TS1-g2s** and **TS1-anr**) and the barriers for the corresponding bond rotations. The barriers for C4−C6 bond rotation through **TS-rot2** and **TS-rot3** (see Scheme 2) were estimated by scan calculations choosing the dihedral angle τ as the selected coordinate. The maxima of these scans are ca. 6 kcal/mol higher than the **IN-g2s** and **IN-anr** intermediates, the corresponding geometries presenting a unique imaginary frequency associated with the dihedral angle τ. Therefore, since the barriers for the bond rotation are higher than that for the dissociation process (ca. 1.2 kcal/mol), the **IN-g2s** and **IN-anr** intermediates are merely in an equilibrium of association and dissociation and only

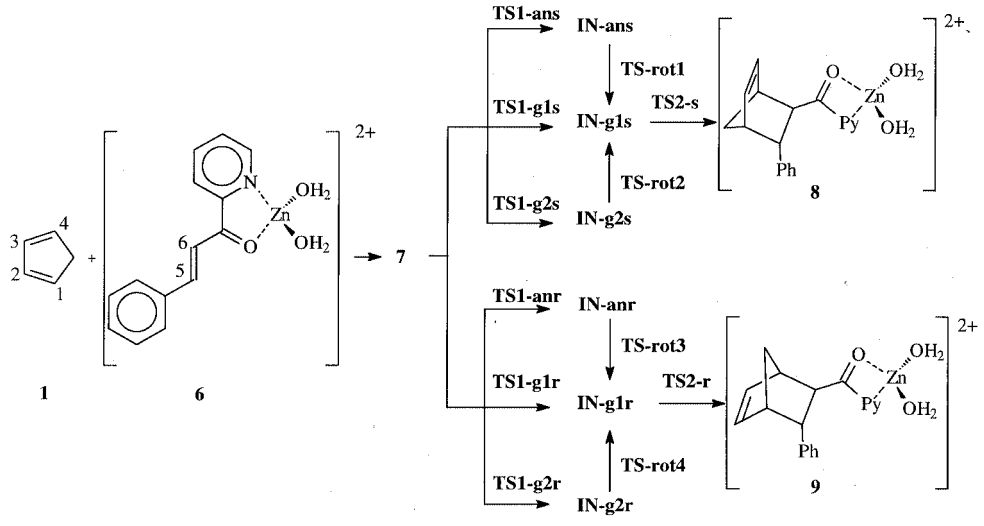

Scheme 2

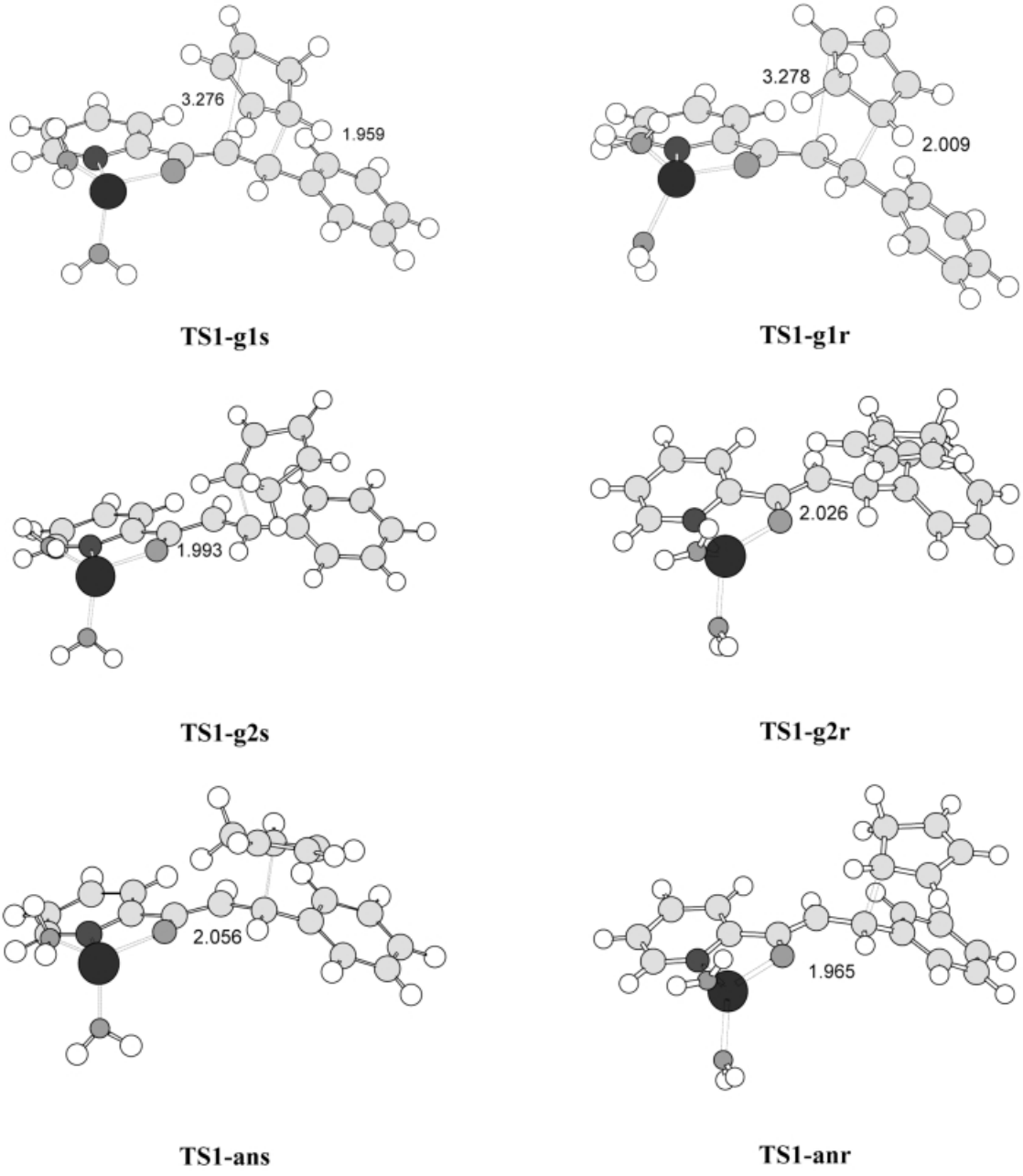

Figure 3. Selected geometrical parameters for the transition structures corresponding to the one-center addition of cyclopentadiene, **1**, to the Zn^{2+} LA-coordinated unsaturated ketone **6**; the lengths of the bonds directly involved in the reaction are given in angstroms

the *g1s* and *g1r* reactive channels are capable of operating in this stepwise cycloaddition. The barrier heights for the LA-catalyzed cycloaddition with respect to **7** are between 11 and 12 kcal/mol. Thus, in the gas phase, the presence of an LA decreases the barrier for the catalyzed process by ca. 10 kcal/mol with respect to the uncatalyzed process.

The lengths of the forming C1−C5 bonds in the TSs corresponding to the one-center addition are in the narrow range of 1.95−2.05 Å, while the distances between the C4 and C6 atoms in **TS1-g1s** and **TS1-g1r** are ca. 3.3 Å. The τ dihedral angles (C2−C1−C5−C6) for the TSs corresponding to the one-center addition are: −66.2° (**TS1-g1s**), 78.2° (**TS1-g2s**), 177.4° (**TS1-ans**), 65.1° (**TS1-g1r**), −73.0° (**TS1-g2r**), and 170.5° (**TS1-anr**) (see Scheme 3). These values correspond to the three staggered conformations of **1** relative to **6** around the forming C1−C5 bond. Analysis of the atomic motion along the unique imaginary frequency associated with these TSs showed that they are mainly associated with the motion of the C1 and C5 carbon atoms during the C1−C5 bond-formation process, in agreement with one-center addition.

In order to understand the factors influencing the heights of the activation barriers of the one-center additions we analyzed the electronic structures of the different TSs. Analysis of the geometries of the more favorable **TS1-g2s** and **TS1-anr** showed that they correspond to the approach of

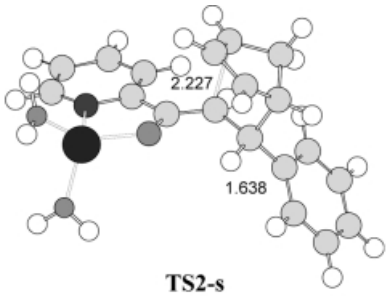

TS2-s

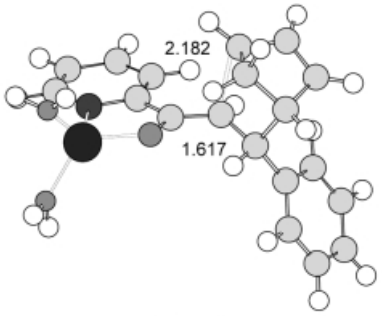

TS2-r

Figure 4. Selected geometrical parameters for the transition structures corresponding to the ring-closure process of the intermediates **IN-g1s** and **IN-g1r**; the lengths of the bonds directly involved in the reaction are given in angstroms

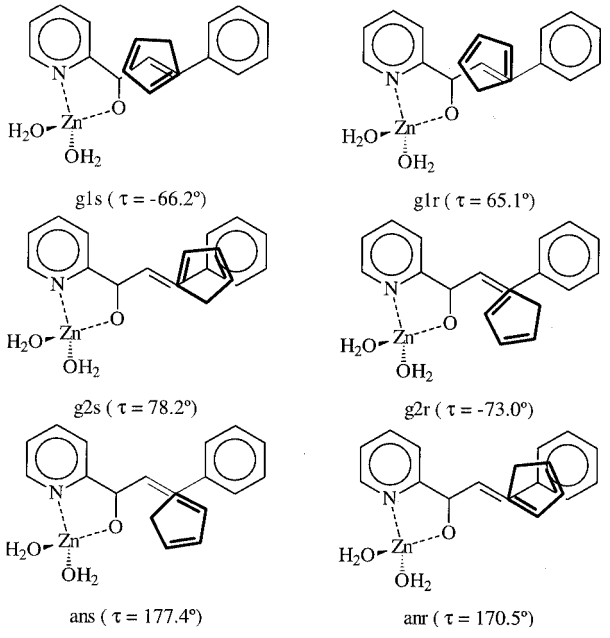

Scheme 3. *gauche* and *anti* arrangements of cyclopentadiene relative to the Zn^{2+} LA-coordinated unsaturated ketone **6** at the TSs associated with the one-center addition

the π-system of the allylic cation moiety of **1** over the π-system of the phenyl substituent present at the C5 position of **6** (see *g2s* and *anr* in Scheme 3). A molecular orbital analysis of these TSs showed the presence of a favorable interaction between the π-system of the allylic cation in **1** and the π-system of the neighboring phenyl framework in **6**. This interaction allows a stabilization of the positive charge developing on the cyclopentadiene during the nucleophilic attack (see later NPA analysis). In addition, the stronger interaction at **TS1-g2s** than at **TS1-anr** explains why **TS1-g2s** is 0.8 kcal/mol lower in energy than **TS1-anr**.

In the corresponding acyclic intermediates, the values of the C1−C5 bond lengths are in the 1.6−1.7 Å range, while the C4−C6 distances in **IN-g1s** and **IN-g1r** have values of 3.478 and 3.242 Å, respectively, indicating that the C4 and C6 atoms are not bonding. The C2−C3 and C3−C4 bond lengths in these intermediates (ca. 1.4 Å) agree with an allylic arrangement for the C2−C3−C4 framework belonging to the cyclopentadiene residue.[14] In the TSs corresponding to the ring-closure process (**TS2-s** and **TS2-r**), the lengths of the forming C4−C6 bonds are 2.227 and 2.182 Å, respectively. Analysis of the atomic motion along the unique imaginary frequency of these TSs indicated that they are mainly associated with the motion of the C4 and C6 carbon atoms during the C4−C6 bond-formation process.

For the TSs corresponding to the nucleophilic attack of **1** at **6**, the BO values for the forming C1−C5 bond are ca. 0.5, while the BO values between the C4 and C6 atoms in **TS1-g1s** and **TS1-g1r** are 0.0. These data indicate that only the C1−C5 bond is being formed in these TSs. The BO values of the C1−C5 bonds in the corresponding intermediates (ca. 0.8) indicate that these C−C single bonds are already formed,[14b] whereas the C4−C6 BO values in the *g1* intermediates **IN-g1s** and **IN-g1r** remain at 0.0. In these intermediates, the BO values for the C2−C3 and C3−C4 bonds (ca. 1.5 and 1.4, respectively) point to an allyl structure for the C2−C3−C4 framework, allowing a favorable stabilization of the positive charge developed on the cyclopentadiene moiety during the nucleophilic attack.[14b] Finally, for the TSs corresponding to the ring-closure processes **TS2-s** and **TS2-r**, the BO values of the forming C4−C6 bonds are ca. 0.4.

NPA allowed us to evaluate the charge transferred during this polar stepwise process, the atomic charges being shared between the donor cyclopentadiene and the acceptor Zn^{2+}-coordinated unsaturated ketone **6**. The negative charge transferred from **1** to **6** in the one-center TSs and corresponding intermediates during the nucleophilic attack is ca. 0.5 e and 0.7 e, respectively. These data show a large increase in the charge transfer in the catalyzed process with respect to the uncatalyzed one. Thus, the role of the LA catalyst in the reduction of the barrier height can be understood as a large increase in the electrophilicity of the LA-coordinated unsaturated ketone,[15] favoring cycloaddition by a polar bond-formation process.[5a,14b] Finally, analysis of the charge transfer in the more favorable TSs for the one-center additions (0.51 e in **TS1-g1s**, 0.55 e in **TS1-g2s**, 0.50 e in **TS1-g1r**, and 0.54 e in **TS1-anr**) shows a greater charge

transfer in the more favorable **TS1-g2s** and **TS1-anr** due to the π-π interactions present in the *g2s* and *anr* arrangements (see Scheme 3).

Study of the Solvent Effects on the Cycloadditions Between 1 and 2 and Between 1 and 6

Recent studies carried out for cycloaddition reactions of strongly polar character have indicated that the inclusion of solvent effects on the geometry optimization does not substantially modify the gas-phase geometries.[14,15a] In consequence, solvent effects were considered by single-point calculations at the gas-phase optimized geometries, with the aid of a relatively simple self-consistent reaction field (SCRF) method[22] based on the polarizable continuum model (PCM) method of Tomasi.[23] Table 1 reports the total and relative energies of the stationary points corresponding to the uncatalyzed and Zn^{2+}-catalyzed cycloaddition reaction between **1** and **2** in water.

The inclusion of solvent effects results in a greater stabilization of the stationary points corresponding to the Zn^{2+}-catalyzed process (between 155 and 190 kcal/mol) than of those for the uncatalyzed one (between 11 and 16 kcal/mol), due to the cationic character of the former. On inclusion of solvent effects the separated reactants are stabilized preferentially, this stabilization being greater for the catalyzed process due to the presence of positive charge on the Zn^{2+}-coordinated ketone **6**. As a consequence, the inclusion of water as a continuum model notably increases the barrier height with respect to the separated reactants for the catalyzed reaction. Similar results have been found for other cationic cycloadditions, in which the inclusion of solvent effects markedly increases the barriers relative to those found in the gas phase.[14] Nevertheless, if we consider the formation of the MCs, the barrier for the LA-catalyzed process remains ca. 10 kcal/mol lower than that for the uncatalyzed one (see Table 1). The increase in the barrier height for the catalyzed process with the inclusion of water can be explained by the strong charge transfer found in the TSs and intermediates, which decreases the solvation with respect to the separated reactants **1** + **6** and the MC **7**. This behavior can explain the unexpectedly weak effect of the water solvent in these cationic LA-catalyzed cycloadditions, and contrasts with the suggestion of Engberts et al. that changes in charge separation during the activation process of the catalyzed reaction are not significantly larger than the corresponding changes in the uncatalyzed process.[10]

Water stabilizes **TS1-g1s** and **TS1-g1r** more effectively than **TS1-g2s** and **TS1-anr** corresponding to the one-center addition, and so only the *g1s* and *g1r* reactive channels are operative in these stepwise processes. Finally, in water, the catalyzed cycloaddition is slightly more *endo*-stereoselective than its uncatalyzed counterpart. These results are in agreement with the experimental observation that water does not induce a clear enhancement of *endo* selectivity for these reactions.[10]

Conclusions

The molecular mechanisms of the uncatalyzed and the Zn^{2+} LA-catalyzed Diels−Alder reactions between cyclopentadiene and 3-phenyl-1-(2-pyridyl)-2-propen-1-one in water have been characterized by quantum mechanical calculations at the B3LYP/6-31G * level of theory. For the uncatalyzed cycloaddition, two reactive channels, *endo* and *exo*, on the PES were characterized, the mechanism corresponding with an asynchronous concerted reaction associated with a [4+2] process. The presence of an LA catalyst changes the mechanism drastically, the reaction now taking place by a polar stepwise process. The first step is the nucleophilic attack of the cyclopentadiene at the conjugate position of the Zn^{2+} LA-coordinated unsaturated ketone to give an acyclic zwitterionic intermediate. Because of the prochiral nature of the carbon atoms involved in the one-center addition and the free rotation of the forming C−C bond, six pairs of enantiomeric reactive channels with similar energies are possible. Because of the large energies required for bond-rotation in the intermediates formed in the first step, however, only the *g1s* and *g1r* reactive channels are capable of operating in this stepwise cycloaddition. A ring-closure process from the corresponding intermediates produces the final *endo* and *exo* formal [4+2] cycloadducts. Finally, water, modeled by a continuum model, has only a weak solvent effect on the barrier height for the Zn^{2+} LA-catalyzed cycloaddition relative to that obtained in the gas phase, and does not induce a clear enhancement of the *endo* selectivity relative to the uncatalyzed process.

Experimental Section

Computational Methods and Models

DFT calculations were carried out with the B3LYP[16] exchange-correlation functional, together with the standard 6-31G* basis set.[17] The optimizations were carried out by the Berny analytical gradient optimization method.[18] The stationary points were characterized by frequency calculations in order to verify that the transition structures had one, and only one, imaginary frequency. The electronic structures of the stationary points were analyzed by the natural bond orbital (NBO) method.[19] All calculations were carried out with the Gaussian 98 suite of programs.[20]

Since the LA-catalyzed reaction presented asynchronous TSs and acyclic intermediates, diradical structures could, in principle, have been involved. This was ruled out by determination of the wave functions of the TSs and intermediates by unrestricted DFT theory. UB3LYP/6-31G* calculations, using the keyword STABLE in Gaussian 98, predicted the same structures as those obtained from the restricted B3LYP/6-31G* calculations, indicating that the restricted DFT solutions were stable, and thus allowing the presence of diradical species to be ruled out.[5a,6,21]

The solvent effects of the water were examined by B3LYP/6-31G* single-point calculations at the gas-phase stationary points involved in the reaction with the aid of a relatively simple SCRF[22] based on Tomasi's group's PCM.[23] We used the dielectric constant of water at 298.0 K; $\varepsilon = 78.39$.

Two models were selected. The first one corresponded to the uncatalyzed reaction between **1** and **2** (see Scheme 1); for this molecular system no restriction has been done. In the second model, the influence of the LA catalyst was then modeled, taking into account the formation of a complex between the carbonyl oxygen and the pyridyl nitrogen atoms of the bidentate **2** and the Zn^{2+} cation. Two discrete water molecules were included around this cation to complete the coordination sphere of four[11] (compound **6**, Scheme 2).

Acknowledgments

This work was supported by research funds provided by the Ministerio de Educación y Cultura of the Spanish Government by DGICYT (project PB98-1429 and PB96-0795-C02-02). All calculations were performed on a Cray-Silicon Graphics Origin 2000 at the Servicio de Informática de la Universidad de Valencia and on two Silicon Graphics Power Challenger L at the Servei d'Informática of the Universitat Jaume I. We are most indebted to these centers for providing us with computer facilities. C. N. A. thanks the Universitat Jaume I for financial support during his stay at this University.

[1] [1a] W. Carruthers, *Some Modern Methods of Organic Synthesis*, second ed., Cambridge University Press: Cambridge, 1978. [1b] W. Carruthers, *Cycloaddition Reactions in Organic Synthesis*, Pergamon: Oxford, 1990. [1c] H. B. Kagan, O. Riant, *Chem. Rev.* **1992**, *92*, 1007−1029. [1d] U. Pindur, G. Lutz, C. Otto, *Chem. Rev.* **1993**, *93*, 741−761. [1e] C.-J. Li, *Chem. Rev.* **1993**, *93*, 2023−2035.

[2] [2a] F. Fringuelli, O. Piermatti, F. Pizzo, L. Vaccaro, *Eur. J. Org. Chem.* **2001**, 439−455. [2b] L. F. Tietze, G. Kettschau, *Top. Curr. Chem.* **1997**, *189*, 1−120. [2c] A. Kumar, *Chem. Rev.* **2001**, *101*, 1−19.

[3] D. A. Singleton, S. R. Merrigan, B. R. Beno, K. N. Houk, *Tetrahedron Lett.* **1999**, *40*, 5817−5821.

[4] [4a] D. M. Birney, K. N. Houk, *J. Am. Chem. Soc.* **1990**, *112*, 4127−4133. [4b] J. Gonzalez, K. N. Houk, *J. Org. Chem.* **1992**, *57*, 3031−3037. [4c] W. L. Jorgensen, D. Lim, J. F. Blake, *J. Am. Chem. Soc.* **1993**, *115*, 2936−2942. [4d] W.-M. Dai, C. W. Lau, S. H. Chung, D.-Y. Wu, *J. Org. Chem.* **1995**, *60*, 8128−8129. [4e] J. González, T. Sordo, J. A. Sordo, *J. Mol. Struct., (Theochem)* **1995**, *358*, 23−27. [4f] J. I. García, J. A. Mayoral, L. Salvatella, *J. Am. Chem. Soc.* **1996**, *118*, 11680−11681. [4g] A. Venturini, J. Joglar, S. Fustero, J. Gonzalez, *J. Org. Chem.* **1997**, *62*, 3919−3926. [4h] A. Sbai, V. Branchadell, R. M. Ortuño, A. Oliva, *J. Org. Chem.* **1997**, *62*, 3049−3054. [4i] J. I. García, V. Martínez-Merino, J. A. Mayoral, L. Salvatella, *J. Am. Chem. Soc.* **1998**, *120*, 2415−2440.

[5] [5a] L. R. Domingo, M. Arnó, J. Andrés, *J. Org. Chem.* **1999**, *64*, 5867−5875. [5b] L. R. Domingo, A. Asensio, *J. Org. Chem.* **2000**, *65*, 1076−1083. [5c] L. R. Domingo, A. Asensio, P. Arroyo, *J. Phys. Org. Chem.* **2002**, in press.

[6] S. Yamabe, T. Minato, *J. Org. Chem.* **2000**, *65*, 1830−1841.

[7] [7a] J. F. Blake, W. L. Jorgensen, *J. Am. Chem. Soc.* **1991**, *113*, 7430−7432. [7b] M. F. Ruiz-López, X. Assfeld, J. I. García, J. A. Mayoral, L. Salvatella, *J. Am. Chem. Soc.* **1993**, *115*, 8780−8787. [7c] M. M. Davidson, I. H. Hillier, R. J. Hall, N. A. Burton, *J. Am. Chem. Soc.* **1994**, *116*, 9294−9297. [7d] C. Cativiela, V. Dillet, J. I. García, J. A. Mayoral, M. F. Ruiz-López, L. Salvatella, *J. Mol. Struct., (Theochem)* **1995**, *331*, 37−50. [7e] C. Cativiela, J. I. García, J. A. Mayoral, L. Salvatella, *Chem. Soc. Rev.* **1996**, *25*, 209−218.

[8] S. Otto, J. B. F. N. Engberts, *Pure Appl. Chem.* **2000**, *72*, 1365−1372.

[9] [9a] S. Otto, J. B. F. N. Engberts, *Tetrahedron Lett.* **1995**, *36*, 2645−2648. [9b] S. Otto, J. B. F. N. Engberts, *J. Am. Chem. Soc.* **1999**, *121*, 6798−6806.

[10] S. Otto, F. Bertoncin, J. B. F. N. Engberts, *J. Am. Chem. Soc.* **1996**, *118*, 7702−7707.

[11] C. N. Alves, A. B. F. da Silva, S. Martí, V. Moliner, M. Oliva, J. Andrés, L.R. Domingo, *Tetrahedron* **2002**, *58*, 2695−2700.

[12] [12a] R. G. Parr, W. Yang, *Density Functional Theory of Atoms and Molecules*; Oxford University Press: New York, 1989.[12b]T. Ziegler, *Chem. Rev.* **1991**, *91*, 651−667.

[13] K. B. Wiberg, *Tetrahedron* **1968**, *24*, 1083−1096.

[14] [14a] L. R. Domingo, *J. Org. Chem.* **2001**, *66*, 3211−3214. [14b] L. R. Domingo, M. Oliva, J. Andrés, *J. Org. Chem.* **2001**, *66*, 6151−6157.

[15] [15a] L. R. Domingo, *Tetrahedron* **2002**, *58*, 3765−3774. [15b] L. R. Domingo, M. J. Aurell, P. Pérez, R. Contreras, *Tetrahedron* **2002**, *58*, 4417−4423.

[16] [16a] A. D. Becke, *J. Chem. Phys.* **1993**, *98*, 5648−5652. [16b] C. Lee, W. Yang, R. G. Parr, *Phys. Rev. B* **1988**, *37*, 785−789.

[17] W. J. Hehre, L. Radom, P. v. R. Schleyer, J. A. Pople, *Ab initio Molecular Orbital Theory*, Wiley: New York, 1986.

[18] H. B. Schlegel, *Geometry Optimization on Potential Energy Surface*, in *Modern Electronic Structure Theory* (Ed.: D.R. Yarkony), World Scientific Publishing: Singapore, 1994.

[19] [19a] A. E. Reed, R. B. Weinstock, F. Weinhold, *J. Chem. Phys.* **1985**, *83*, 735−746. [19b] A. E. Reed, L. A. Curtiss, F. Weinhold, *Chem. Rev.* **1988**, *88*, 899−926.

[20] M. J. Frisch, G. W. Trucks, H. B. Schlegel, G. E. Scuseria, M. A. Robb, J. R. Cheeseman, V. G. Zakrzewski, J. A. Montgomery, J., R. E. Stratmann, J. C. Burant, S. Dapprich, J. M. Millam, A. D. Daniels, K. N. Kudin, M. C. Strain, O. Farkas, J. Tomasi, V. Barone, M. Cossi, R. Cammi, B. Mennucci, C. Pomelli, C. Adamo, S. Clifford, J. Ochterski, G. A. Petersson, P. Y. Ayala, Q. Cui, K. Morokuma, D. K. Malick, A. D. Rabuck, K. Raghavachari, J. B. Foresman, J. Cioslowski, J. V. Ortiz, B. B. Stefanov, G. Liu, A. Liashenko, P. Piskorz, I. Komaromi, R. Gomperts, R. L. Martin, D. J. Fox, T. Keith, M. A. Al-Laham, C. Y. Peng, A. Nanayakkara, C. Gonzalez, M. W. Challacombe, P. M. Gill, B. Johnson, W. Chen, M. W. Wong, J. L. Andres, C. Gonzalez, M. Head-Gordon, E. S. Replogle, J. A. Pople, Gaussian 98, Revision A.6 Gaussian, Inc.: Pittsburgh PA, 1998.

[21] S. D. Kahn, W. J. Hehre, J. A. Pople, *J. Am. Chem. Soc.* **1987**, *109*, 1871−1873.

[22] [22a] O. Tapia, *J. Math. Chem.* **1992**, *10*, 139−181. [22b] J. Tomasi, M. Persico, *Chem. Rev.* **1994**, *94*, 2027−2094. [22c] B. Y. Simkin, I. Sheikhet, *Quantum Chemical and Statistical Theory of Solutions-A Computational Approach*, Ellis Horwood: London, 1995.

[23] [23a] M. T. Cances, V. Mennunci, J. Tomasi, *J. Chem. Phys.* **1997**, *107*, 3032−3041. [23b] M. Cossi, V. Barone, R. Cammi, J. Tomasi, *Chem. Phys. Lett.* **1996**, *255*, 327−335. [23c] V. Barone, M. Cossi, J. Tomasi, *J. Comp. Chem.* **1998**, *19*, 404−417.

Received January 31, 2002
[O02055]